Diffusion-Drift Modeling of Carbon-Based Nanowire FETs

M.G. Ancona and J.B. Boos
Electronics S&T Division
Naval Research Laboratory
Washington, DC, USA
ancona@estd.nrl.navy.mil

***Abstract*—Continuum models of transport in carbon nanotubes and graphene nanoribbons are created by treating the charge flow in the carbon layers in a 2D diffusion-drift approximation. A crucial element of the treatment is the electron equation of state that allows the effects of confinement and chirality to be represented. To model nanowire devices, the transport layer is embedded within a 3D structure and coupled to the electrostatics. This is illustrated with applications to carbon-based nanowire field-effect transistors of varying designs.**

Keywords—diffusion-drift; carbon nanotubes, graphene nanoribbons; field-effect transistors.

I. Introduction

Switching devices composed of semiconducting single-wall carbon nanotubes (CNTs) have received much attention and remain promising despite the continued lack of convenient means for controlling their diameter, chirality, and placement [1]. A second and less advanced carbon-based approach is that involving devices composed of graphene nanoribbons (GNRs) [2]. Essentially all prior work aimed at numerically simulating the behavior of such carbon-based nanowire devices has employed microscopic approaches with the non-equilibrium Green's function (NEGF) method being most popular [3,4]. As a complementary approach, we here investigate doing such modeling using macroscopic methods like diffusion-drift (DD) theory that experience has shown are often of value from an engineering perspective.

When developing a detailed continuum description of a CNT or GNR device it is important to recognize that the simplest idea of modeling them as 1D line segments is untenable because of well known singularities that occur in the electrostatics of line charges. Consequently, we intead formulate our classical field descriptions of carbon-based nanowire FETs by treated the CNTs or GNRs explicitly as 2D objects in much the same manner as in the DD theory of graphene [5]. Apart from the obvious change in geometry, the main difference from the graphene theory is in the equations of state of the carrier gases that are modified to account for effects of the confinement and chirality. The system of differential equations is completed by embedding the 2D transport equations in a 3D electrostatics problem. Lastly, to formulate boundary value problems a consistent set of boundary conditions is needed, and in the case of CNTs these are identical to those used in [5]. For GNRs there is the additional complication of the "lateral" edges whose properties depend on the orientation, e.g., armchair or zigzag edges, and on edge disorder and termination [6]. In this paper we focus on armchair GNRs for which there are no conducting states at the edge and the behavior is similar to that of a quantum well. In the continuum theory we represent this behavior using a density-gradient (DG) approach [7]. The latter might also be used to model source-drain tunneling effects [7], however this not considered in the present paper. Similarly, another phenomenon associated with scaling not treated here is ballistic transport effects.

II. Theory

Semiconducting CNTs and GNRs have significant bandgaps, a feature that stands in contrast to the parent material of graphene and that is crucial to the field-effect devices that are the focus of this paper. It also means that one can often consider only one carrier type unlike with graphene. In particular, we here focus on n-channel devices and so need only equations describing electron transport. These equations assume steady-state conditions and utilize either the DD or the "DGC" version of the DG approximations. These equations represent a basic assumption that the transport is scattering-dominated.

A. Differential Equations and Boundary Conditions

The 2D DD transport equations for graphene of [5], when generalized to include possible DG terms [7], take the form:

$$(1a) \qquad \nabla_s \cdot \bar{\boldsymbol{J}}^n = 0 \qquad \bar{\boldsymbol{J}}^n = \bar{\mu}_n \bar{n} \nabla_s \bar{\Phi}^n$$

$$(1b) \qquad \frac{1}{\bar{s}} \nabla_s \cdot (b_n \nabla_s \bar{s}) = \bar{\Phi}^n - \psi + \bar{\varphi}^n(\bar{n})$$

where over-bars indicate 2D variables, ∇_s is the surface gradient operator, $\bar{s} \equiv \sqrt{\bar{n}}$, and the DD description results when the DG coefficient b_n is set to zero. In this paper, we assume either planar or cylindrical coordinates, but more general 2D geometries (e.g., for a deformed CNT or a helical GNR [8]) could also be considered. As indicated, the electron chemical potential $\bar{\varphi}^n(\bar{n})$ is a function of the 2D electron density, and as discussed in the next sub-section its specification is crucial to a proper description of the carbon materials. Lastly, with no volumetric space charge in the system, the 3D electrostatic equation obeys:

The authors thank the Office of Naval Research for funding support.

978-1-4673-7860-4/15/$31.00 ©2015 IEEE

(2) $$\nabla \cdot (\varepsilon_d \nabla \psi) = 0$$

As in [5], the most important boundary condition of the theory is the electrostatic one across the carbon layer which takes the form:

(3) $$\mathbf{n} \cdot \left(\varepsilon_{d(2)} \nabla \psi^{(2)} - \varepsilon_{d(1)} \nabla \psi^{(1)} \right) = q(\bar{n} - \bar{N}_D)$$

where $\mathbf{n}$ is the normal vector to the layer pointing from the (1) side to the (2) side and $\bar{N}_D$ is the donor dopant concentration which is often remote in such devices. Ohmic boundary conditions are assumed at the source and drain contacts and the side edges of the GNRs are assumed insulating.

B. Electron Equation of State

For the CNT and GNR models to be accurate it is essential that the electron gas response be well represented by an appropriate equation of state as expressed by the function $\bar{\varphi}^n(\bar{n})$. According to equilibrium statistical mechanics the chemical potential will be implicitly related to the density of 2D conduction states $g(E)$ by the Fermi-Dirac integral:

(4) $$\bar{n}(\bar{\varphi}^n) = \int_{E_C}^{\infty} \frac{g(E)\, dE}{1 + exp\left[\frac{E - \bar{\varphi}^n}{kT}\right]}$$

To make use of this expression microscopic models for $g(E)$ in CNTs and in GNRs are needed.

In the case of CNTs we base the equation of state on the understanding derived from the graphene sheet model (GSM) [9] that ignores the effects of CNT curvature. As examples, the equations of state for the electrons in semiconducting CNTs with chiralities of (5,0), (10,0), (20,0) and (16,8) are plotted in Fig. 1; it should be noted that the GSM result for the (5,0) CNT is known to be inaccurate because of its extreme curvature.

In contrast, an armchair GNR is effectively a graphene quantum well, and so as in the analogous treatment of a semiconductor quantum well [7], we simply use the graphene equation of state discussed previously in [5]. The situation of zigzag GNRs, where there is the added complication of conducting edge states, is not analyzed here.

C. Numerics

As with any classical field description, application of the foregoing equations proceeds by formulating boundary value problems appropriate to the devices of interest. The CNTs are modeled as cylindrical tubes, whereas the GNRs are modeled as narrow strips. Because of the complexity of the equations of state we do attempt to develop analytical representations, and instead simply resort to look-up tables. The numerical formulations are standard, and the solutions are obtained using the Comsol FEM package (see www.comsol.com).

III. Carbon Nanotube FETs

We illustrate the macroscopic transport description of a CNT FET by considering a device whose channel consists of a single semiconducting CNT. In the device, the CNT is situated on an SiO_2-coated substrate, which is then covered with a second insulator (whose properties may vary) and the gate electrode. We assume the CNT to be laterally centered, so that symmetry allows the representation to be halved as depicted in Fig. 2. No attempt is made to model the complex physics of the source/drain contacts; instead they are treated simply as ideal n+ doped regions, which implies that we consider a CNT FET that is channel-dominated rather than one whose

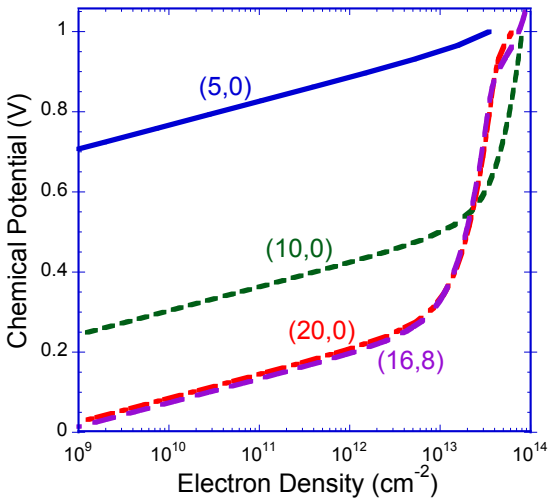

Fig. 1. Equations of state for semiconducting CNTs of varying chiralities.

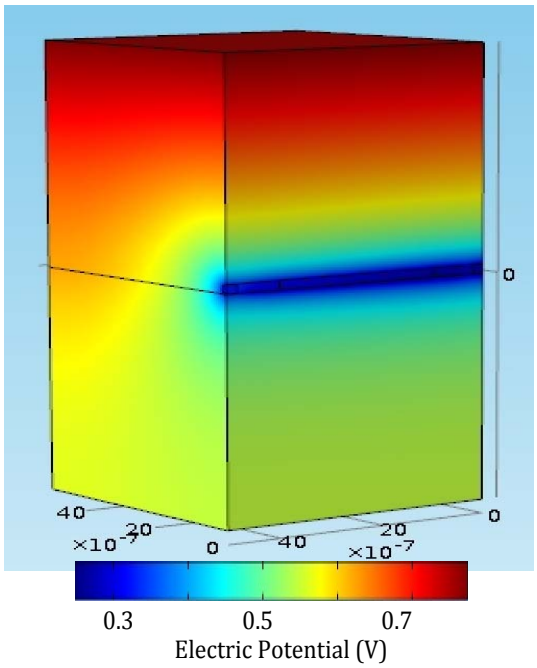

Fig. 2. Section from FET geometry that is symmetric about the vertical plane on the right. The gate electrode is on the top surface and the CNT is located on the midline.

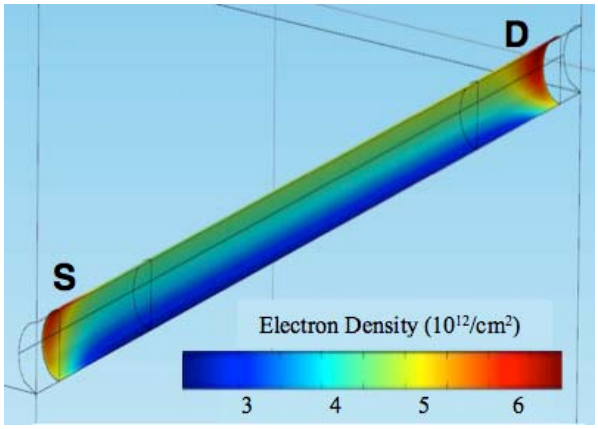

Fig. 3. Simulated electron density in a (16,8) CNT with V_G = 0.5V and V_{SD} = 50mV.

transport properties are dictated by its Schottky contacts.

For illustration we consider the specific case of a (16,8) CNT, and in Fig. 3 display the solution for the electron density in the CNT with clear circumferential asymmetry due to the gate bias. In Fig. 4 we plot the gate capacitance versus gate voltage assuming the gate insulator is SiO_2, HfO_2, or a fictional insulator with a dielectric constant of 250. As is well known, the latter "impossible" situation results in the total capacitance being dominated by the CNT's space-charge component.

The simulated transfer and drain characteristics of a (16,8) CNT FET are plotted in Figs. 5a and 5b with curves shown for the three insulators analyzed in Fig. 4. The higher levels of current are simply the result of the increased capacitance as plotted in Fig. 4. Carrying out many such simulations could allow device concepts such as that presented in [10] for a CNT-based linear amplifier to be evaluated in the scattering-

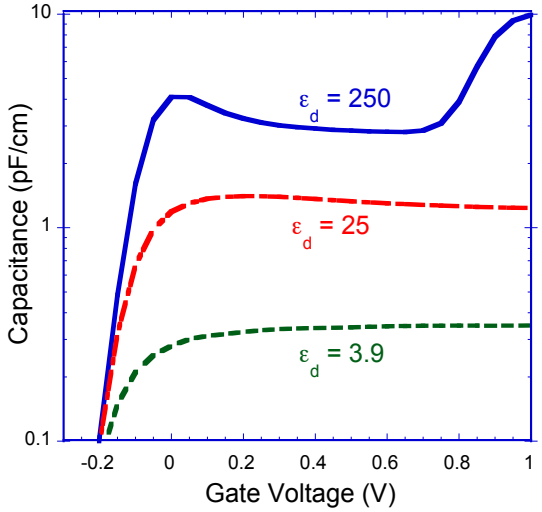

Fig. 4. Gate capacitance with ε_d as a parameter. Topmost curve is dominated by space-charge capactitance with the shape due to subband structure.

dominated regime. In this regard, that the data in Fig. 5a, when plotted linearly, show very little improvement in linearity as the dielectric constant increases suggests that the inherent linearity expected in [10] will not be met when scattering is important.

IV. Graphene Nanoribbon FETs

As our second example of carbon-based nanowire modeling we discuss the simulation of GNR FETs using the DG equations. A crucial parameter in these simulations is the value of the DG effective mass in the confinement direction. As discussed in [7], when the confinement is strong as it would be in a narrow GNR, then the best accuracy is obtain when DG theory is treated as a phenomenology with the DG mass determined, for example, by curve-fitting NEGF results. A

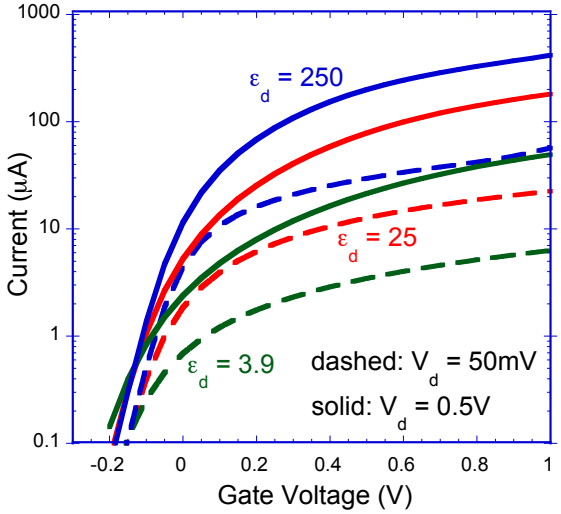

Fig. 5a. Transfer characteristics for various gate dielectrics and at two drain voltages.

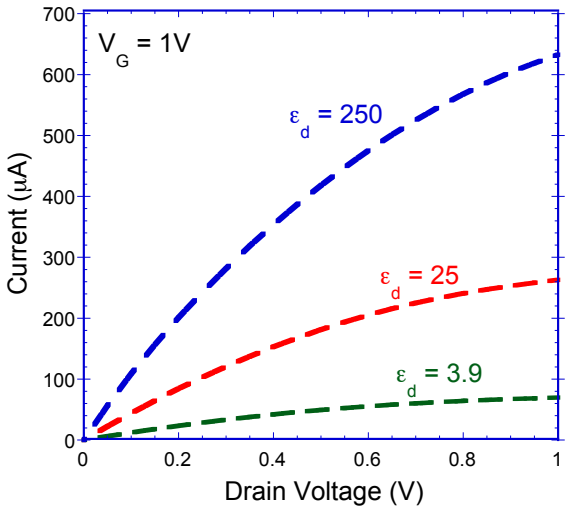

Fig. 5b. Drain characteristics of a (15,8) CNT FET with varying gate dielectrics.

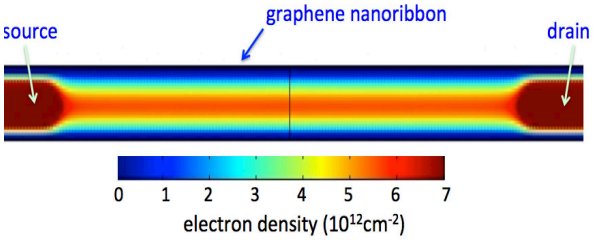

Fig. 6a. Density variation inside a 5nm wide graphene nano-ribbon. The effect of the confinement is evident.

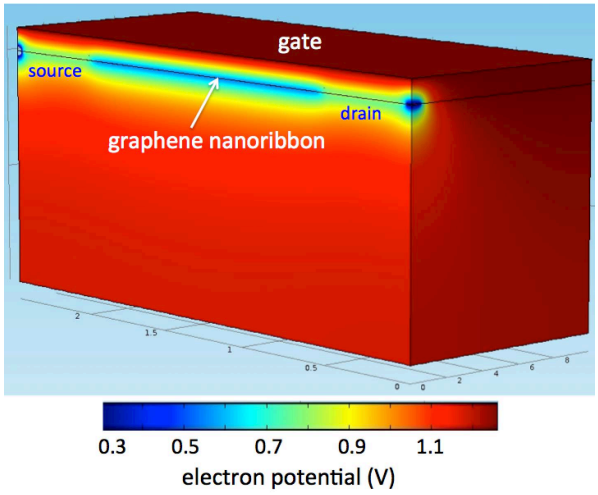

Fig. 6b. Electric potential in a GNR FET.

crude version of this has been employed here where we fit the two-band model of [6] and take $m_e^{DG} \approx 0.018 m_e$.

Two illustrative results from the DG simulations of a GNR FET are shown in Figs. 6a and 6b. The GNR is 5nm wide GNR and the strong confinement of the electron density is evident in Fig. 6a. The field concentration produced by the narrow GNR is seen in the plot of the electric potential in Fig. 6b.

V. Final Remarks

The capacity for simulating carbon-based nanowire FETs in the scattering-dominated regime using macroscopic methods has been demonstrated. Both classical (DD) and quantum (DG) transport theories have been used and the crucial step was to represent the nanowire channel as a 2D object embedded in a 3D electrostatics. This was exhibited with two examples, namely CNT and GNR FETs. It is important to recognize that the results given here are of qualitative value only, and to develop faith in them in a quantitative sense would require significant effort of validation. Much as was done in [5] and [7] this would involve careful comparisons between the continuum simulations and results obtained both experimentally as in [1] and [2] and from microscopic simulations such as those of [3], [4] and [6].

References

[1] G.S. Tulevski, A.D. Franklin, D. Frank, J.M. Lobez, Q. Cao, H. Park, A. Afzali, S.-J. Han, J.B. Hannon, and W. Haensch, "Toward high-performance digital logic technology with carbon nanotubes," *ACS Nano* **8**, 8730 (2014).

[2] X. Wang, Y. Ouyang, X. Li, H. Wang, J. Guo, and H. Dai, "Room-temperature all-semiconducting sub-10nm graphene nanoribbon field-effect transistors," *Phys. Rev. Lett.* **100**, 206803 (2008).

[3] Y. Ouyang, Y. Yoon, J.K. Fodor, and J. Guo, "Comparison of performance limits for carbon nanoribbon and carbon nanotube transistors," Appl. Phys. Lett. 89, 203107 (2006).

[4] G. Fiori and G. Iannaccone, "Multiscale modeling for graphene-based nanoscale transistors," *Proc. IEEE* **101**, 1653 (2013).

[5] M.G. Ancona, "Electron transport in graphene from a diffuson-drift perspective," *IEEE Trans. Elect. Dev.* **57**, 681 (2010).

[6] D. Gunlycke and C.T. White, "Scaling of the localization length in armchair-edge graphene nanoriboons," *Phys. Rev.* **81**, 075434 (2010).

[7] M.G. Ancona, "Density-gradient theory: A macroscopic approach to quantum confinement and tunneling in semiconductor devices," *J. Comput. Electron*. **10**, 65-97 (2011).

[8] D. Gunlycke, J. Li, J.W. Mintmire, and C.T. White, "Edges bring new dimension to graphene nanoribbons," *Nano Lett.* **10**, 3638 (2010).

[9] C.T White and J.W. Mintmire, "Fundamental properties of single-wall carbon nanotubes," *J. Phys. Chem. C* **109**, 89 (2005).

[10] J.E. Baumgardner *et al*., "Inherent linearity in carbon nanotube field-effect transistors," *Appl. Phys. Lett*. **91**, 052107 (2007).